

A Multispectral Acquisition System using MSFAs

Pierre-Jean Lapray; University of Burgundy; Dijon, France
Jean-Baptiste Thomas; University of Burgundy; Dijon, France
Pierre Gouton; University of Burgundy; Dijon, France

Abstract

Thanks to technical progress in interferential filter design, we can finally implement in practice the concept of Multispectral Filter Array based sensors. This article presents the characteristics of the elements of our sensor as a case study. The spectral characteristics are based on two different spatial arrangements that distribute eight different bandpass filters in the visible and near-infrared area of the spectrum. We demonstrate that the system is viable and evaluate its performance through sensor spectral simulation and characterization.

Introduction

In digital color imaging, the concept of Color Filter Array (CFA) has been exploited since the 1970s and the invention of the Bayer pattern [1]. Indeed, at the expense of spatial resolution, one can increase the spectral resolution of an imaging device.

While multispectral imaging is now a solution commonly considered for several problems and applications, *i.e.* medical imaging and cultural heritage, there is still the need to develop a compact and affordable solution. The complexity and need of tunability of such multispectral imaging device limit its use to some specialized area and often requires experts to handle them.

MultiSpectral Filter Arrays (MSFAs), could provide an easier, compact, general and affordable solution, such as CFAs do to digital color cameras. A synopsis of the MSFA concept is shown in Figure 1. Some attempts deal in simulation with the problem of spatial distribution [12], demosaicing [11, 18, 25], image processing [5, 16, 19] or compression [17]. However, only a few works provide a practical implementation of the concept, due to technical difficulties to realize filter arrays of a size of a few micrometers to match pixels. Although there exist a long list of technology that permits snapshot multispectral imaging, only a few considers the practical implementation of general purpose MSFAs [6, 13]. One only deals with the fusion of an RGB and a Near-Infrared (NIR) sensors, the other tends to have more filters and is closer to the solution we propose.

These works could allow development of general purpose, fast, multispectral and spatially accurate imaging through the use of video analysis [2], with potential applications in robotics, quality, monitoring, etc.

This paper provides a practical demonstration of the sensor we are developing at the University of Bourgogne. The paper is organized as follows: we first provide a narrow state of the art of snapshot Multispectral imaging technologies, we then analyze our system by showing our sensor and filters spectral sensitivities. Next, we show and analyze the two spatial arrangements that we use, we relate their size with the pixel size of the sensor. Finally, we show what we can do with our customized electronics and

software.

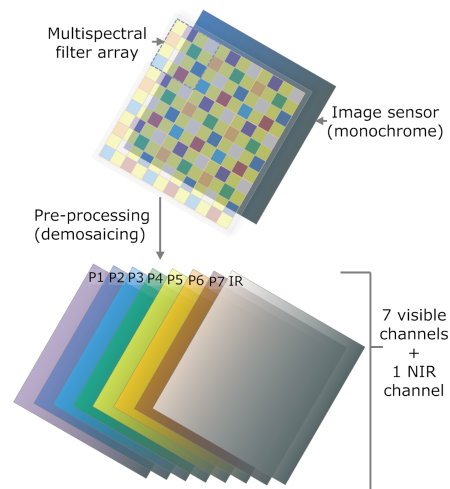


Figure 1. Global scheme of the multispectral imaging system based on MSFAs. The filter array is mounted on a common CMOS image sensor.

MSFAs snapshot multispectral imaging

Although there exist a few practical realizations of this technology, little results have been reported on the pre-processing of experimental data (denoising, demosaicing, etc.).

To fabricate the 128-band MSFA [24], Wang *et al.* develop a technique named combinatorial deposition [23] that combines the techniques of deposition and etching in order to produce the spacer arrays with different thickness required by the corresponding Fabry-Pérot type filter element. Such a device makes possible *in situ* spectral measurement of NIR spectra ranging from 722 nm to 880 nm. The fabrication is suitable for direct integration onto CMOS image sensors in industrial foundries, and the cost and complexity is reduced in comparison with other solutions that vary the physical cavity length only. Another Fabry-Pérot interferometer based snapshot multispectral imager is developed by Gupta *et al.* [7]. The imager employs a 16-band MSFA arranged in 4×4 moxels that operate in the short wavelength infrared range from 1487 to 1769 nm with a spectral bandpass of about 10 nm. The MSFA is installed in a commercial handheld InGaAs camera coupled with a customised micro-lens array with telecentric imaging performance in each of the 16 channels.

A paper by Qi [15] presents an implementation of multispectral array filters, composed of 4 narrow-band cells at 540, 577, 650 and 970nm. Their implementation is a practical application dedi-

cated to early detection of pressure ulcer. The filter mosaic is fabricated by combining the lift-off process in microstructuring and thin film coating technology through physical vapor deposition. They use a conventional Aptina imager, and due to hard manufacturing process, each cell of the filter cover 16 pixels of the full raw image. They propose a software processing in order to avoid two type of degradations: the misalignment between filter and the sensor, and the reconstruction of missing spectral components (demosaicking). The implementation results show some success and promises a real-time production of multispectral images that allows instant detection.

A significant study conducted by Harvard University [13, 14], offers multispectral mosaiced filters based on nanowires. A wavelength-selective coupling to the guided nanowire mode is used in order to capture 8 sampled multispectral images from visible (3 bands) and NIR (5 bands) wavelength. A polydimethylsiloxane (PDMS) film is mounted directly on a CCD monochrome sensor. They show particular image experiments dedicated to Normalized Difference Vegetation Index imaging.

Sensor and filter analysis

Silicon sensors typically respond to incident radiation in the visible and NIR range of the spectrum. Thus, we designed MSFAs to capture wavelengths between 400 nm and 1100 nm in the visible range and the NIR range. Our solution combines a standard sensor built on CMOS technology, with customized filters. This section presents the spectral characteristics of these two components.

The CMOS sensor is a Sapphire EV76C661 from e2v [4]. It offers a 10-bit digital readout speed at 60 frames per second (fps) with full resolution. This sensor provides relatively good sensitivity in NIR spectrum ($> 50\%$ at 860 nm) while keeping good performance in the visible spectrum (quantum efficiency $> 80\%$). Due to relatively low transmission factors of the filters, it is important, in our case, to have a good pixel sensor quantum efficiency. It can tolerate more noise, and is favorable for low-light sensing. The sensor also embeds some basic image processing functions such as image histograms, defective pixel correction, evaluation of the number of low and high saturated pixels, etc. Each frame can be delivered with results of these functions encoded in the image data stream header. The resolution of the sensor is 1280×1024 . We measured its sensitivity with a monochromator (OL Series 750 Spectroradiometric Measurement System [21]) by sweeping the wavelength of the light from the monochromator from 400 nm to 1100 nm by steps of 10 nm. A tungsten light source is used to have the tunable light source. The power supply of the light source and the wavelength of the monochromator are controlled by computer. The sensor is used without any lens mounted in front of the camera. The formula used to recover the quantum efficiency (Q_E) is as follows in Equation 1:

$$Q_E(\lambda) = \frac{hc \times D_i(\lambda)}{I(\lambda) \times \lambda \times \Delta t \times S_{e2v}}, \quad (1)$$

where h is the Planck constant, c the speed of light in vacuum, λ the wavelength, Δt the exposure time used for characterization, D_i the digital intensity, I the irradiance at a specific wavelength and S_{e2v} the area of an effective sensor pixel. The value of the pixels from the image captured by the e2v sensor at each wavelength is recorded. We find the relative sensor response, which is shown in

Figure 2. This same experimental setup is used to characterize the complete system in terms of sensitivity of spectral channels.

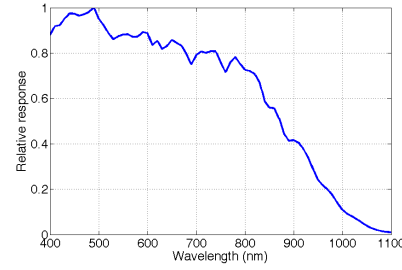


Figure 2. Relative response of the e2v EV76C661ABT sensor [4]. The measurements were done by using the OL Series 750 Spectroradiometric Measurement System [21] with a tungsten lamp.

Our customized matrix of filters is built by SILIOS technologies [22]. SILIOS Technologies developed the COLOR SHADES technology, allowing the manufacture of multi-spectral filters. COLOR SHADES technology is based on the combination of thin film deposition and micro-/nano-etching processes onto fused silica substrate. Standard micro-photolithography steps are used to define the cell geometry of the multi-spectral filter. COLOR SHADES provides band pass filters originally in the visible range from 400 nm to 700 nm. Through our collaboration, SILIOS developed filters in the NIR range, combining their technology with a classical thin layer interferential technology to realize our filters.

The theoretical and experimental transmittances of the filters are shown on Figure 3. The filters are 8 bands, $\{P1, P2, P3, P4, P5, P6, P7, IR\}$. We show difference between expected values previously calculated on simulation, and experimental values after filter fabrication. Table 1 presents the center wavelengths, the width of each filters at mid-level (FWHM), and the maximum transmissions of filters.

Table 1. Optical specification of filter bands (theoretical and practical).

Band	Center Wavelength (nm)		FWHM (nm)		Max. Transmission (%)	
	Sim.	Result	Sim.	Result	Sim.	Result
P1	420	427	35	38	70	47
P2	465	467	26	31	64	50
P3	515	510	23	28	61	52
P4	560	561	21	26	56	54
P5	609	605	19	25	57	49
P6	645	654	18	24	62	47
P7	700	699	15	22	69	45
IR	> 865	> 885	-	-	> 75	> 75

Compared to the theoretical responses expected on Figure 3(a), we can see that the maximum transmittances decrease in the extreme parts of the visible spectrum. The peak sensitivities did not move too much. Two major differences appear on the IR spectral response:

1. The IR-cut is centred on 885nm instead of 865nm ,

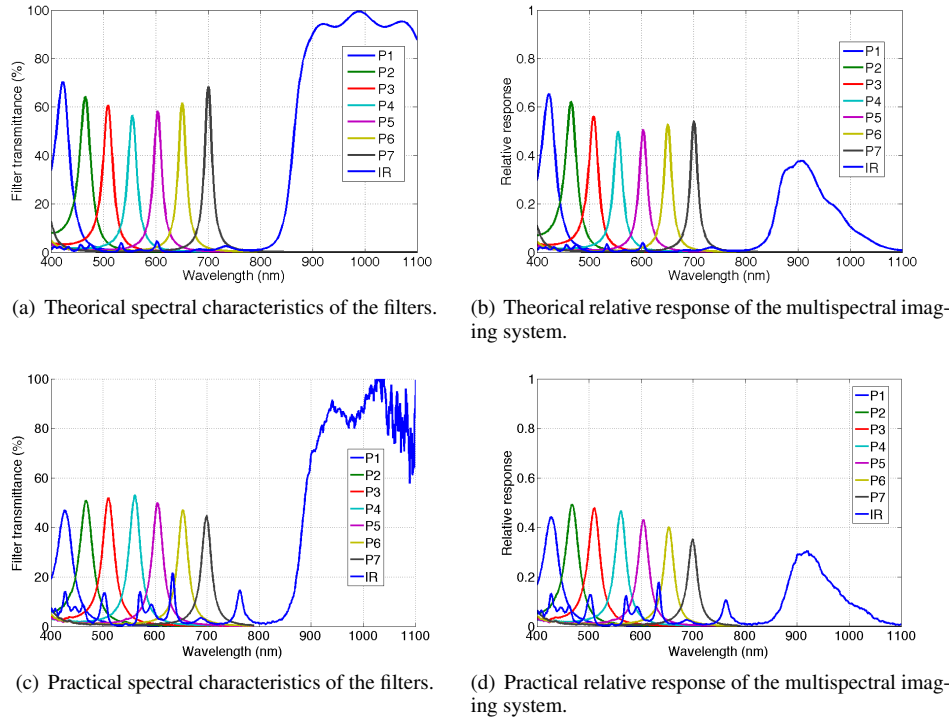


Figure 3. (a) Simulation of the spectral characteristics of the selected filters. Channels $\{P1 - P7; IR\}$, are labelled following the scheme of Figure 4. (b) Simulation of the relative actual response of the multispectral imaging system (sensor associated with filters). (c) Measure of the spectral characteristics of the selected filters. We note that the efficiency in the visible is less than planned and, more critically, that the IR filters contains a larger part of the visible signal. (d) Actual response of the multispectral imaging system (sensor associated with filters)

2. The IR rejection is worse than expected with one peak at 20% and 4 peaks at 10% in the visible. The transmittances in the visible range is due to manufacturing problems. Indeed, the process is very complicated when you need area of a few microns, parasites and inefficient areas can occur.

The NIR filter has a specific shape since it is based on classical thin layer interferential filters. We can see that the shape of the filters acts like an additive component, where specific wavelength are added through gaussian-like shapes.

Unfortunately, we could not reach a very good cut off in the visible range for our IR filter. This will impact the sensitivity of the final sensor in two ways: First, the IR channel will contains visible information if there is no post processing involved. However, since we have information within the visible range, up to 780 nm, it is possible to include a software dynamic correction to the IR channel, which will then contains information captured only along the last part of the filter. Second, the energy balance of the sensor can be critically affected (see next section).

After fabrication, multispectral filters are mounted on the image sensor directly on the microlens array. Figures 3(d) and 3(b) show the MSFA sensor sensitivities (simulation and actually measured), that combine the CMOS sensor and our filters.

Spatial arrangements

This section considers the size and spatial arrangement of the mosaic of filters.

Arranging the MSFA pattern is a major challenge. Beside the method proposed by Miao *et al.* [11], the distributions are usually ad hoc or the result of an optimization process [10]. So are the arrangements of our filters. We defined two different spatial distributions corresponding to two different characteristics. One is favoring the spatial information, and the other one the spectral information. FS1 offers an over-sampled spatial information of two spectral bands. P5 is designed as the green channel in a Bayer

Table 2. Relative normalized values of the sensor response (ρ_{P_N}) by filter for a given input illuminant and a perfect diffuser.

Illuminant	E	D65	A
$R_{Sinarback}$	0.47	0.41	0.68
$G_{Sinarback}$	1	1	1
$B_{Sinarback}$	0.82	0.85	0.48
P_1	0.78	0.78	0.25
P_2	0.94	1	0.41
P_3	0.97	0.91	0.58
P_4	1	0.81	0.80
P_5	0.95	0.67	0.90
P_6	0.92	0.56	1
P_7	0.84	0.45	0.99
$IR1(400 - 780nm)$	0.84	0.60	0.71
$IR2(780 - 1100nm)$	2.84	x	x

P5	P1	P5	IR
P6	P5	P4	P5
P5	IR	P5	P2
P3	P5	P7	P5

(a) FS1

P1	P5	P2	P6
P7	P3	IR	P4
P2	P6	P1	P5
IR	P4	P7	P3

(b) FS2

Figure 4. Filter arrangements defined in this work. The distributions FS1 (a) and FS2 (b) are repeated up to the limits of the sensor. See Figure 3(a) for spectral characteristics of the filter channels.

CFA, and IR is double-sampled compared with the rest of the filters. Such arrangement is supposed to provide a good spatial reconstruction and reasonably good information in the NIR domain. FS2 is designed to have a sub-sampled spatial information for the benefit of a more important spectral information. This filter is designed following the method proposed by Miao *et al.* [11] with equal probability of occurrence of each channel. The filter arrangements chosen are shown in Figures 4(a) and 4(b).

The sensor pixel pitch is $5.3 \mu m$, but each filter element measures $21.2 \times 21.2 \mu m^2$, corresponding to 4×4 sensor pixels. The sensor is populated by 1280×1024 pixels. The actual resolution of the filter mounted sensor is then equal to 320×256 pixels. The total filter matrix size is $6.78 \times 5.43 mm^2$. Additionally, a margin is introduced in order to support mechanical switching during assembly, that is why the total carrier physical size is $6.9 \times 5.6 mm^2$. About the alignment and assembly of the filters with the sensor pixel matrix, alignment matrices are drawn in the corners of the filters. These areas occupy 16×16 pixels in the four corners of the physical matrix. These matrices are designed with solid color and chrome patterns for tracking. Figure 5 shows one of these matrices.

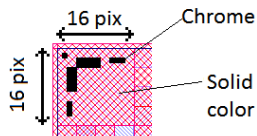


Figure 5. One alignment matrix, in the top left corner of the filter array.

To test the geometric/algebraic structure of the sampling patterns of the MSFAs FS1 and FS2, we analyze spatial subsampling through a log-magnitude representation of channels of the Skauli Stanford Tower image [20] (see Figure 6). The radiance data cover wavelengths from $415 nm$ to $950 nm$ in steps of approximately $3.65 nm$, spanning the visible and NIR spectral ranges. The image is processed as it simply simulates an acquisition by our sensor. Figure 6(b) illustrates the facts that we have one pixel in two on the P5 channel of pattern FS1 (Nyquist frequency). Figure 6(c) shows we have one pixel in two in diagonal for most of the channels of our array. On Figure 6(d), we can observe the sparser sampling of most spectral channel of pattern FS1, one sample every four pixels in all the eight directions.

To test the energy balance of our sensor [8], and evaluate its ability to acquire multispectral information in one single shoot,

we compute the convolution, as in Equation 2:

$$\rho_{P_N} = \int_{400}^{780} \text{Illuminant} \cdot R_{e2v} \cdot T_{\lambda, P_N} d\lambda, \quad (2)$$

where $N \in \{1-7\}$, R_{e2v} is the relative response of the single sensor and T_{λ, P_N} is the transmittance of each filter P_N . The convolution results are normalized with the maximum transmittance in the visible for each illuminant. Results are shown in Table 2. We note that the energetic distribution through our filters is reasonably balanced in the visible, since the variance between the spectral bands is acceptable for illuminant E and D_{65} . Results can be compared to the typical curves of the RGB Sinarback camera [3], where the convolution variance is considered to be good enough for sensor energy balance. It is likely that a single exposure is sufficient to capture all spectral bands P1-P7. IR1 in Table 2 shows the addition of a visible component if we simply put an IR cut-off filter on top of the sensor. It demonstrates that the sensor is very good if we only consider the visible range. Exposure setting tests will probably confirm this analysis in future works.

The case of the NIR filter generates more problems. Indeed, the global energy ratio is about 4 times the other channels (3.68), we can expect over-exposed pixels through the IR channel VS under-exposed pixels in the others for a given integration time. It can be avoided by using a specific global filter at a certain wavelength in order to balance the sensor but this is not easy to realise and will cut too much IR information. Experimental results are needed to assess and quantify this problem.

Acquisition and preprocessing

The sensor is controlled by a customized electronic board designed at our Lab and plugged on an FPGA board (see Figure 7(a)). The sensor board and a part of the hardware description previously performed in our laboratory [9] was re-used and updated (sensor configuration, video timing detection/generation and display).

A software developed in our lab (see Figure 7(b)), provides the control of most functions and acquisition of images or video sequences. The software is used to retrieve the video stream from the sensor through the UDP Ethernet protocol. A live preview of the resulting image after demosaicing channels is also available for both arrangements FS1 and FS2. To ensure a high speed and a real-time preview of the result, only a bilinear interpolation demosaicing has been implemented yet. On block 1 and 2, we can see the preview of the image acquired on a selected channel. This is very convenient to focus on a specific filter depending on the pattern used (*i.e.* the P5 channel of FS1). Block 4 permits us to configure the sensor (exposure time) and to perform video acquisition or snapshot. Block 3 is a tool to perform the spectral calibration with a monochromator.

Full resolution channel interpolations dedicated to our spatial arrangement and spectral characteristics must be considered to ensure a better image quality. The reduced spatial image resolution is a typical problem of CFAs and MSFAs due to their intrinsic property that a certain spectral band is allocated specifically at each location of the array. Due to the manufacturing constraints, $16 (4 \times 4)$ photosensitive elements on the sensor correspond to one filter. Therefore pre-processing becomes necessary to recover the information of each band to a certain extent, known as demosaicing. In fact, standard techniques will fail to reconstruct consis-

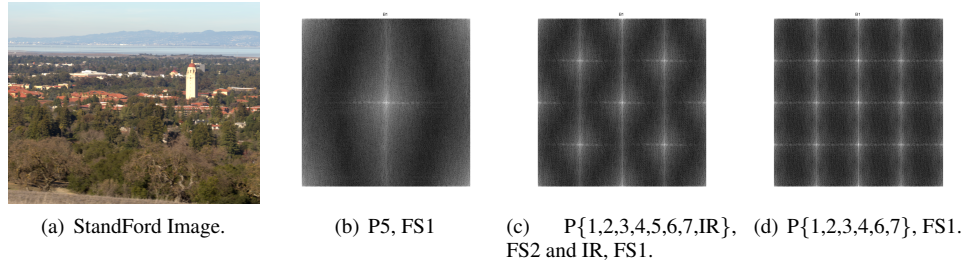


Figure 6. (a) Multispectral image by Skauli [20] is used. (b, c, d) Log-magnitude representation of spatial arrangement for channels of both FS1 and FS2. This is simply the sampling rate of the filters in the Fourier domain.

tently all the derived images due to the large gap across edges. Such a technique should be fast enough to handle video processing, while having a good accuracy in the color plane reconstruction. This problem will be addressed in further communications.

Conclusions

This work establishes a consistent design of MSFAs based imaging sensor, from elaboration to pre-implementation. Two filters are to be implemented on a standard 1.3 megapixel sensor. The filters are constructed on a 2D substrate, so that different wavelengths of light can be captured simultaneously as we can do with Bayer filter. We posed 2 MSFAs designs formally in order to test both the maximization of the spectral and spatial information. Our simulation with several illuminants seems to indicate that it will not be necessary to use multiple exposure acquisition for the visible range, but this can be more critical for the NIR channel. Also, the NIR filter does not cut perfectly the visible part of the spectrum and we expect to need more pre-processing if it is required by the application. Finally, the manufacturing process is relatively simple and reproducible. The resulting system is small compared to the existing multispectral vision systems.

We suggest that such a very general sensor can still be tuned (by adding an IR-cut filter for instance) for a given application, and could serve as a future ground for general multi-component imaging purpose.

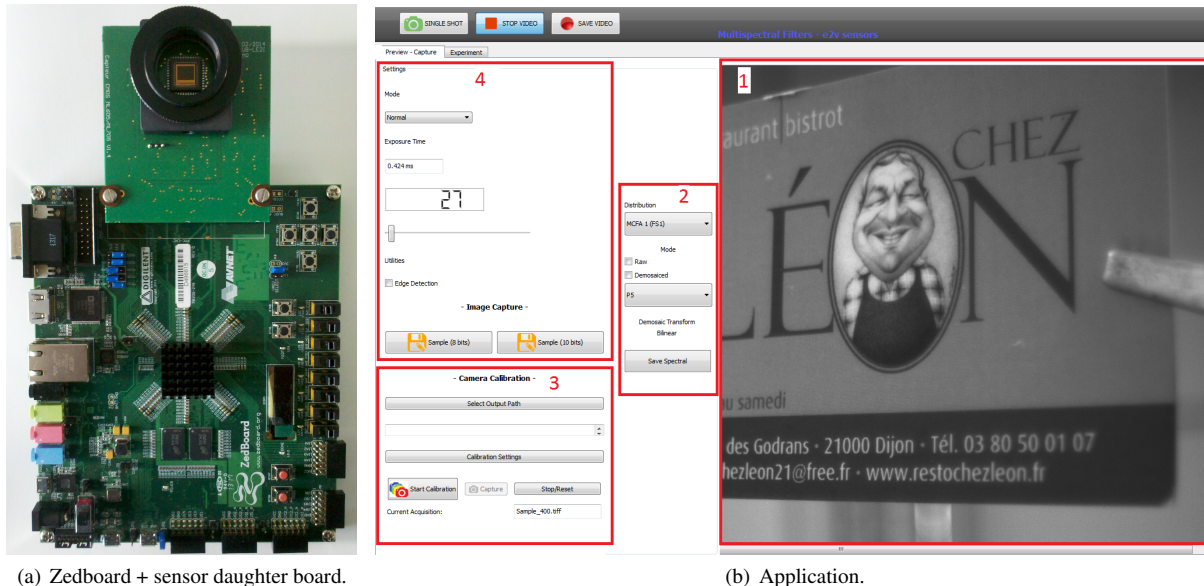
Further investigations and adjustments are needed. Specifically, we are interested in the development of dedicated demosaicing algorithms. On the other hand, a huge amount of work will be required to investigate cross-talk effects between filter cells.

Acknowledgments

The authors wish to thank Xingbo Wang for his comments and for sharing helpfull software tools, and Matthieu Rossé for the design of electronics. The authors thanks the Open Food System project for funding. Open Food System is a research project supported by Vitagora, Cap Digital, Imaginove, Aquimer, Microtechnique and Agrimip, funded by the French State and the Franche-Comt Region as part of The Investments for the Future Programme managed by Bpifrance, www.openfoodsystem.fr.

References

- [1] Bryce E. Bayer. Color imaging array. Patent, 07 1976. US 3971065.
- [2] Yannick Benezeth, Désiré Sidibé, and Jean-Baptiste Thomas. Background subtraction with multispectral video sequences. In *IEEE ICRA workshops*, page 6 p., Hong-Kong, 2014.
- [3] DAY D.C. Spectral sensitivities of the sinarback 54 camera. Technical report, Spectral Color Imaging Laboratory Group Munsell Color Science Laboratory Chester F. Carlson Center for Imaging Science Rochester Institute of Technology, February 2003.
- [4] e2v technologies. Ev76c661 BW and colour CMOS sensor, 2009. www.e2v.com.
- [5] Chen Feng, Shaojie Zhuo, Xiaopeng Zhang, Liang Shen, and Sabine Ssstrunk. Near-Infrared Guided Color Image Dehazing. In *Proc. IEEE 20th International Conference on Image Processing (ICIP)*, pages 2363 – 2367, 2013.
- [6] Clement Fredembach, Yue M. Lu, and Sabine Susstrunk. Camera design for the simultaneous capture of near-infrared and visible images. Patent US8462238, 2013.
- [7] Neelam Gupta, Philip R. Ashe, and Songsheng Tan. Miniature snapshot multispectral imager. *Optical Engineering*, 50(3):033203–033203–9, 2011.
- [8] Péguillet Hugues, Jean-Baptiste Thomas, Pierre Gouton, and Yasmine Ruichek. Energy balance in single exposure multispectral sensors. In *Colour and Visual Computing Symposium (CVCS), 2013*, pages 1 – 6, Gjøvik, Norvège, September 2013.
- [9] Pierre-Jean Lapray, Barthélémy Heyrman, and Dominique Ginjac. Hdr-artist: An adaptive real-time smart camera for high dynamic range imaging. *Journal of Real-Time Image Processing*, pages 1–16, January 2014.
- [10] Yue M. Lu, Clément Fredembach, Martin Vetterli, and Sabine Ssstrunk. Designing color filter arrays for the joint capture of visible and near-infrared images. In *Proceedings of the 16th IEEE International Conference on Image Processing, ICIP'09*, pages 3753–3756, Piscataway, NJ, USA, 2009. IEEE Press.
- [11] Lidan Miao, Hairong Qi, R. Ramanath, and W.E. Snyder. Binary tree-based generic demosaicking algorithm for multispectral filter arrays. *Image Processing, IEEE Transactions on*, 15(11):3550–3558, Nov 2006.
- [12] Lidan Miao, Hairong Qi, and W.E. Snyder. A generic method for generating multispectral filter arrays. In *Image Processing, 2004. ICIP '04. 2004 International Conference on*, volume 5, pages 3343–3346 Vol. 5, Oct 2004.
- [13] Hyunsung Park and Kenneth B Crozier. Multispectral imaging with vertical silicon nanowires. *Scientific reports*, 3, 2013.
- [14] Hyunsung Park, Yaping Dan, Kwanyong Seo, Young J Yu, Peter K Duane, Munib Wober, and Kenneth B Crozier. Vertical silicon nanowire photodetectors: Spectral sensitivity via nanowire radius. In *CLEO: Science and Innovations*, pages CTh3L–5. Optical Society of America, 2013.
- [15] Hairong Qi, Linghua Kong, Chao Wang, and Lidan Miao. A hand-



(a) Zedboard + sensor daughter board.

(b) Application.

Figure 7. Overview of the hardware/software system, with front view of the assembled camera (a), and the control/test application. Application features: 1- Video preview, 2- Channel and filter selection, 3- Characterization tool, 4- Setting tools. An preview after bilinear demosaicing is a functionality of the application.

held mosaicked multispectral imaging device for early stage pressure ulcer detection. *Journal of Medical Systems*, 35(5):895–904, 2011.

- [16] Dominic Rafenacht, Clment Fredembach, and Sabine Susstrunk. Automatic and Accurate Shadow Detection using Near-Infrared Information. *IEEE Transactions on Pattern Analysis and Machine Intelligence*, 2014.
- [17] Zahra Sadeghipoor Kermani, Yue Lu, and Sabine Ssstrunk. A Novel Compressive Sensing Approach to Simultaneously Acquire Color and Near-infrared Images on a Single Sensor. In *Proc. International Conference on Acoustics, Speech, and Signal Processing (ICASSP)*, pages 1646 – 1650, 2013.
- [18] Zahra Sadeghipoor Kermani, Yue Lu, and Sabine Susstrunk. Correlation-based Joint Acquisition and Demosaicing of Visible and Near-Infrared Images. In *IEEE International Conference on Image Processing (ICIP)*, IEEE International Conference on Image Processing ICIP. Ieee Service Center, 445 Hoes Lane, Po Box 1331, Piscataway, Nj 08855-1331 Usa, 2011.
- [19] Neda Salamati, Diane Larlus, Gabriela Csurka, and Sabine Ssstrunk. Semantic Image Segmentation Using Visible and Near-Infrared Channels. In *Lecture Notes in Computer Science*, volume 7584, pages 461–471. Springer Berlin Heidelberg, 2012.
- [20] Torbjrn Skauli and Joyce Farrell. A collection of hyperspectral images for imaging systems research, 2013.
- [21] Optronics OL750 Automated Spectroradiometer. <http://www.photonicsonline.com/doc/ol-series-750-0001>.
- [22] SILIOS TECHNOLOGIES. Micro-optics supplier. <http://www.silios.com/>.
- [23] S.-W. Wang, M. Li, C.-S. Xia, H.-Q. Wang, X.-S. Chen, and W. Lu. 128 channels of integrated filter array rapidly fabricated by using the combinatorial deposition technique. *Applied Physics B*, 88(2):281–284, 2007.
- [24] Shao-Wei Wang, Changsheng Xia, Xiaoshuang Chen, Wei Lu, Ming Li, Haiqian Wang, Weibo Zheng, and Tao Zhang. Concept of a high-resolution miniature spectrometer using an integrated filter ar-

ray. *Opt. Lett.*, 32(6):632–634, Mar 2007.

- [25] Xingbo Wang, Jean-Baptiste Thomas, Jon Yngve Hardeberg, and Pierre Gouton. Median filtering in multispectral filter array demosaicking. In Sebastiano Battiato Nitin Sampat, editor, *Proc. SPIE*, volume 8660, pages Digital Photography IX, 86600E, Burlingame, États-Unis, February 2013.

Author Biography

Pierre-Jean Lapray received his Masters degree in embedded electronics engineering from the Burgundy University. He received his PhD from the Université of Burgundy in 2013. His research interests include image enhancement techniques, embedded systems and real time applications.

Jean-Baptiste Thomas received his Bachelor in Applied Physics in 2004 and his Master in Optics, Image and Vision in 2006, both from the Université Jean Monnet in France. He received his PhD from the Université of Bourgogne in 2009. After a stay as a researcher at the Gjøvik University College and then at the C2RMF (Centre de Recherche et de Restauration des Musées de France), he is now Maître de Conférences (Associate Professor) at the University of Bourgogne. His research focuses on color science and on color and multi-spectral imaging.

Pierre Gouton obtained his Ph.D. in components, signals, and systems at the University of Montpellier (France) in 1991. From 1988 to 1992, he has worked on passive power components at the Laboratory of Electric Machine of Montpellier. Appointed Assistant Professor in 1993 at the University of Burgundy, France, he joined the Image Processing Group of the LE2I (Laboratoire d'Electronique, Informatique et Image: Laboratory of Electronics, Computer Sciences, and Image). Since then, his main research involves the segmentation of images by linear methods (edge detector) or nonlinear methods (mathematical morphology, classification). He is a member of ISIS (a research group in signal and image processing of the French National Scientific Research Committee) and also a member of the French Color Group. Since December 2000, he is an incumbent of the HDR (Habilitation a Diriger les Recherches : Enabling to Manage Researches).